Supporting Information

Nicoll et al. 10.1073/pnas.1009062107

SI Materials and Methods

Materials. Porphyrins were purchased from Frontier Scientific and other reagents from Sigma-Aldrich or Melford. Porphyrins were dissolved from solid into DMSO to a final concentration of 10 mM and dissolved further into buffer as required.

Protein Expression and Purification. Human prion protein $HuPrP_{91–231}$ and $huPrP_{119–231}$ were produced in the *Escherichia coli* strain BL21 DE3 (Novagen) using an isopropyl β-D-1-thio-galactopyranoside-inducible plasmid pTrcHisB (Invitrogen) as described (1). The protein was extracted, refolded, and purified using the method of Zahn et al. (2). Protein quality and purity was confirmed by SDS-PAGE, MALDI-TOF-MS, and CD spectroscopy. Uniformly ^{15}N-labeled $huPrP_{91–231}$ for NMR studies was prepared from M9 minimal media supplemented with ^{15}N ammonium sulfate and purified as normal.

Equilibrium Dialysis. Compounds were diluted from 10 mM DMSO stocks to 100 μM using the same 10 mM Hepes, 25 mM NaCl (pH 7.5) buffer in which the protein had been dialyzed. $HuPrP_{91–231}$ was diluted to 100 μM using identical buffer and 1 vol% DMSO was added to match the compound buffer. Seventy-five microliters of compound solution was added to one chamber of a DispoEquilibrium DIALYZER (Harvard Apparatus) with a 5,000 molecular weight cutoff. Seventy-five microliters of $huPrP_{91–231}$ solution was added to the other chamber and the sample was left to equilibrate at room temperature for 2 d with gentle rocking. After this time, 50 μL of sample was removed and diluted in 150 μL of buffer and the UV-visible spectra were recorded on a Jasco V-530 UV-visible spectrometer in a Hellma ultramicro cuvette with either buffer or protein backgrounds subtracted. Compounds that had failed to equilibrate by this time were assumed to form large, colloidal aggregates. Compounds which fully equilibrated with equal amounts of compound in each chamber were assumed not to bind to PrP, whereas those which concentrated in the protein-containing chamber were assumed to interact and were analyzed further.

Isothermal Titration Calorimetry (ITC). Titrations were performed on a VP-ITC (MicroCal) (3). HuPrP was dialyzed against 10 mM Hepes, 25 mM NaCl (pH 7.5) overnight, filtered through a 0.22 μm filter, and its concentration determined using the calculated extinction coefficient (4). Generally, huPrP was diluted to 10–50 μM with dialysis buffer then DMSO added to give a final concentration of 5 vol%. Porphyrins were dissolved in the same stock of DMSO to give a final concentration of approximately 10 mM before diluting in dialysis buffer to give a final DMSO concentration of 5 vol%. Where 150 mM NaCl was used, a reduced DMSO concentration of 1 vol% was used to prevent porphyrin aggregation under the combined conditions of high porphyrin concentration, high ionic strength, and high DMSO concentration. Solutions were temperature equilibrated and degassed for 5 min prior to loading the protein into the calorimeter cell and the porphyrin into the syringe. Data were recorded with a background of 10 μcal/s at 25 °C, a stirrer speed of 303 rpm, and with deionized water in the control cell. After an initial delay of 240 s, a 2 μL injection was made followed by 14 further 20 μL injections 240 s apart. Data were automatically collected and analyzed using a one-site model in the Origin software (version 7.0) provided by MicroCal with endpoint ligand dilution effects subtracted. For the reverse paradigm, protein was concentrated to 460 μM and Fe(III)-TMPyP diluted to 40.5 μM. The cell and syringe were cleaned between runs with 5% SDS and extensively washed with water.

Circular Dichroism Spectroscopy. Induced CD studies were performed on a Jasco J715 spectropolarimeter in a 10 mm cuvette. Fe(III)-TMPyP was diluted to 18 μM in buffer (10 mM Hepes, 25 mM NaCl (pH 7.5), 1 vol% DMSO) from a 9 mM DMSO stock. Spectra were run between 550–250 nm and were the average of 10 scans. Dissociation constants were calculated for individual experiments using the induced CD at 420 nm in Grafit 5 by fitting a one-site Langmuir isotherm. CD denaturation experiments were performed with the aid of a Jasco peltier temperature control system in a 10 mm cuvette. $HuPrP_{91–231}$ was diluted to 6.5 μM in buffer (10 mM Hepes, 25 mM NaCl (pH 7.5), 5 vol% DMSO) with the sample heated at 1 °C/ min between 20–80 °C and signal measured at 235 nm. The T_m was calculated by fitting the curve to the Van't Hoff equation.

Sedimentation Velocity Analytical Ultracentrifugation. Experiments were performed on a Beckman XLI analytical ultracentrifuge fitted with an An50-Ti rotor in quartz cells containing two-sector centerpieces. Samples were prepared with different PrP and Fe(III)-TMPyP concentrations in 10 mM Hepes, 25 mM NaCl (pH 7.5), 5 vol% DMSO. Samples were centrifuged at an average $193{,}000 \times g$ and 20 °C, and absorbance data were collected at both 278 and 420 nm over 16 h, typically with scans recorded every 10 min. Sedimentation velocity data at 278 and 420 nm were analyzed separately using the $c(s)$ distribution method in the software SEDFIT (version 11.3) (5). For the analyses, partial specific volume ($\bar{\nu}$) for $huPrP_{91–231}$ was calculated from the amino acid sequence using the software SEDNTERP (6), and buffer densities and viscosities were measured using an Anton Paar DMA5000 density meter and an Anton Paar AMVn automated microviscometer, respectively. The proportion of small molecule forming a complex with the protein was calculated from the relative occupancy of the peak at ~1.7 Svedberg in the 420 nm dataset. Dissociation constants were calculated for individual experiments in Grafit 5 using a one-site Langmuir isotherm.

Nuclear Magnetic Resonance Spectroscopy. NMR spectra were acquired at 298 K on a Bruker DRX-600 spectrometer equipped with a 5 mm $^{13}C/^{15}N/^{1}H$ triple-resonance probe. Proton chemical shifts were referenced to 1 mM TSP (trimethylsilyl-2,2,3,3-tetradeuteropropionic acid) added to the samples; ^{15}N chemical shifts were calculated relative to TSP, using the gyromagnetic ratios of ^{15}N and ^{1}H ($^{15}N/^{1}H = 0.101329118$). NMR data were processed and analyzed on Linux Workstations using Felix 2004 (Accelrys) software. Samples of $huPrP_{91–231}$ (200 μM in 20 mM NaAc pH 5.5) were titrated with either apo-TMPyP or Fe(III)-TMPyP from 4 mM stocks in H_2O, by successive additions of 0.2 molar equivalents. At each addition, samples were allowed to equilibrate for 60 min before acquisition of 1D ^{1}H and 2D ^{1}H-^{15}N heteronuclear single quantum coherence (HSQC) spectra. ^{1}H-^{15}N HSQC spectra were acquired using sensitivity-enhanced pulsed field gradient coherence selection (7–9) with acquisition times of 163.4 and 89.7 ms in the ^{1}H and ^{15}N dimensions, respectively. For the Fe(III)-TMPyP titration, the intensities of each resolved HSQC resonance was measured and normalized to the intensity in the absence of compound. For apo-TMPyP, the chemical shifts in both ^{1}H and ^{15}N dimensions were measured.

Computer Modeling. The NMR structure (1QLX) of residues 23–230 of the human prion protein was used for modeling the interaction between PrP^c and Fe(III)-TMPyP. This structure is ordered between residues 125–228. The three missing residues at the C terminus (229–231) were modeled by extending the C-terminal helix. The intensity data (Fig. 3*B*) were displayed on the PrP^c backbone (with color) and used to guide docking of Fe(III)-TMPyP to the C-terminal region of PrP^c by inspection using molecular graphics. The initial model was refined using in-house docking software (10–12). The distribution of attenuated NMR signals expected from this complex was simulated by applying the simple function (1)

$$\begin{aligned}
&\text{dist(Fe,NH}_i) < 13.0\ \text{Å}, \quad I_{\text{HOLO}i} = 0.0 I_{\text{APO}i};\\
&\text{dist(Fe,NH}_i) > 19.0\ \text{Å}, \quad I_{\text{HOLO}i} = 1.0 I_{\text{APO}i};\\
&13.0\ \text{Å} < \text{dist(Fe,NH}_i) < 19.0\ \text{Å},\\
&\quad I_{\text{HOLO}i} = I_{\text{APO}i}(\text{dist(Fe,NH}_i) - 13.0)/6.0, \qquad \textbf{[S1]}
\end{aligned}$$

where $I_{\text{HOLO}i}$ is the signal intensity of residue i in the complex, and $I_{\text{APO}i}$ is the signal intensity of residue i in the free protein.

Cell-Based Prion Curing Assay. Cronically prion-infected N2a cells (subclone "PK1") (13) were cultured in OPTIMEM (Invitrogen) supplemented with 10% FCS (Perbio) and penicillin/streptomycin (Invitrogen). Chronically infected with Rocky Mountain Laboratory (RML) prions, 6,000 cells were seeded into 384-well plates with 50 μL per well of media supplemented with Fe(III)-TMPyP at various concentrations for 3 d before assaying for levels of proteinase K-resistant PrP. Briefly, cells were lysed in ice-cold lysis buffer (50 mM Tris, 150 mM NaCl (pH 7.4), 0.5% Na deoxycholate, 0.5% Triton X-100), blotted onto nitrocellulose membrane in a BioRad 96-well dot blot manifold apparatus, treated in situ with proteinase K (5 μg/mL for 1 h at 37 °C). The reaction was stopped by the addition of 4 mM 4-(2-aminoethyl)benzenesulfonyl fluoride for 15 min , after which the protein was denaturant (3 M guanididium thiocyanate). The membrane was then blocked with Odyssey blocking buffer overnight at 4 °C. Immunodetection was achieved using ICSM 18 (0.2 μg/mL) as a primary antibody and IRDye 800CW goat anti-mouse IgG antibody as a secondary antibody. The membrane was then dried and the proteinase K-resistant PrP ($n = 4$) visualized using an Odyssey scanner and normalized against 100% intensity in untreated control samples. Half-maximal inhibition constants (IC_{50}) were derived by fitting of the averaged and normalized data by using Grafit 5 (Erithacus Software, Ltd). Cytotoxicity was detected using the sensitive ATP-based cell titre-glo luminescence assay (Cell titre-glo, Promega) in duplicate on cells grown at the same time and under identical conditions.

Protein-Misfolding Cyclic Amplification. Protein-misfolding cyclic amplification (PMCA) was performed as described previously (14). Briefly, 10% (wt/vol) PMCA substrate homogenates were prepared from Tg20 mice brains which had been perfused with PBS containing 5 mM EDTA at the time of death. Brains were homogenized in cold conversion buffer [PBS containing 150 mM NaCl, 1.0 vol% Triton X-100, 4 mM EDTA, and Complete Protease Inhibitor Mixture (Roche Applied Biosciences)]. Substrate homogenates were clarified by centrifugation at $1{,}000 \times g$ for 45 sec and then stored at −70 °C without freeze-thawing until required. RML (15) prion-infected homogenate was added to pooled PMCA substrate homogenate at a dilution of 500-fold. The pooled homogenate was split into four separate tubes. In tubes 2 and 3, Fe(III)-TMPyP was added to a final concentration of 11 μm and 1 μM, respectively. Tube 1 was left untouched as a positive control of amplification and, to tube 4, Mn(III)-TMPyP was added to a final concentration of 11 μm as a negative control for inhibition. One-hundred microliter aliquots were taken from each tube and transferred into 0.2 mL PCR tubes and 40 μL retained as minus PMCA controls. Samples were subjected to 85 cycles of PMCA consisting of a 20 s pulse of sonication at 70% power output using a Misonix S4000 sonicator with a microplate horn (Misonix) followed by incubation for 30 min at 35 °C. All samples were analyzed by PK digestion (200 μg/mL final protease concentration for 60 min at 37 °C) and Western blotting. Signal intensity of bands was quantified using ImageMaster 1D Elite software (GE Healthcare Life Sciences). The average amplification for each sample was calculated ($n = 3$) as multiples of control levels and significance was calculated by an unpaired t test (GraphPad InStat).

1. Jackson GS, et al. (1999) Multiple folding pathways for heterologously expressed human prion protein. *Biochim Biophys Acta* 1431:1–13.
2. Zahn R, von Schroetter C, Wuthrich K (1997) Human prion proteins expressed in *Escherichia coli* and purified by high-affinity column refolding. *FEBS Lett* 417:400–404.
3. Wiseman T, et al. (1989) Rapid measurement of binding constants and heats of binding using a new titration calorimeter. *Anal Biochem* 179:131–137.
4. Gasteiger E, et al. (2003) ExPASy: The proteomics server for in-depth protein knowledge and analysis. *Nucleic Acids Res* 31:3784–3788.
5. Schuck P, et al. (2002) Size-distribution analysis of proteins by analytical ultracentrifugation: Strategies and application to model systems. *Biophys J* 82:1096–1111.
6. Laue TM, Shah BD, Ridgeway TM, Pelletier SL (1992) Computer-aided interpretation of analytical sedimentation data for proteins. *Analytical Ultracentrifugation in Biochemistry and Polymer Science.*, eds Harding SE, Horton JC, Rowe AJ (Royal Society of Chemistry, Cambridge, UK), pp 90–125.
7. Bodenhausen G, Ruben DJ (1980) natural abundance N-15 NMR by enhanced heteronuclear spectroscopy. *Chem Phys Lett* 69:185–189.
8. Kay LE, Xu GY, Yamazaki T (1994) Enhanced-sensitivity triple-resonance spectroscopy with minimal H20 saturation. *J Magn Reson Ser A* 109:129–133.
9. Schleucher J, et al. (1994) A general enhancement scheme in heteronuclear multidimensional NMR employing pulsed field gradients. *J Biomol NMR* 4:301–306.
10. Gibbs N, Clarke AR, Sessions RB (2001) Ab initio protein structure prediction using physicochemical potentials and a simplified off-lattice model. *Proteins* 43:186–202.
11. Sessions RB, Thomas GL, Parker MJ (2004) Water as a conformational editor in protein folding. *J Mol Biol* 343:1125–1133.
12. Thomas GL, Sessions RB, Parker MJ (2005) Density guided importance sampling: Application to a reduced model of protein folding. *Bioinformatics* 21:2839–2843.
13. Klohn P, et al. (2003) A quantitative, highly sensitive cell-based infectivity assay for mouse scrapie prions. *Proc Natl Acad Sci USA* 100:11666–11671.
14. Castilla J, et al. (2006) Protein misfolding cyclic amplification for diagnosis and prion propagation studies. *Method Enzymol* 412:3–21.
15. Chandler RL (1961) Encephalopathy in mice produced by inoculation with scrapie brain material. *Lancet* 1:1378–1379.

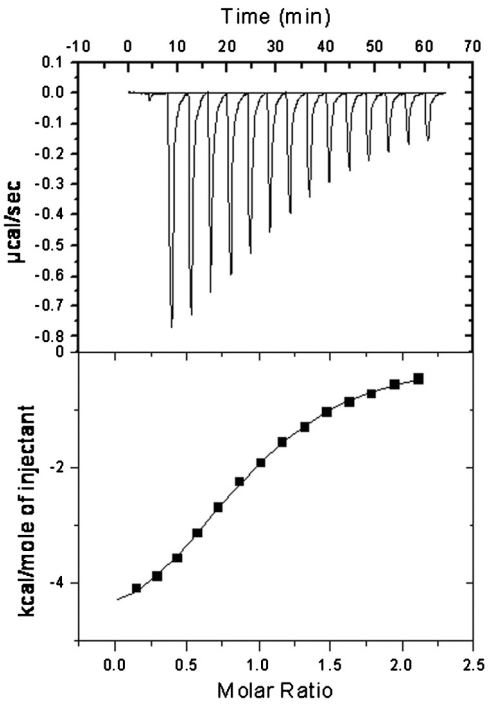

Fig. S1. ITC of Fe(III)-TMPyP injected into huPrP$_{91–231}$ in the presence of 150 mM NaCl. Isotherms for the titration of Fe(III)-TMPyP (500 µM) into huPrP$_{91–231}$ (50 µM) in the presence of 150 mM NaCl, 1% DMSO.

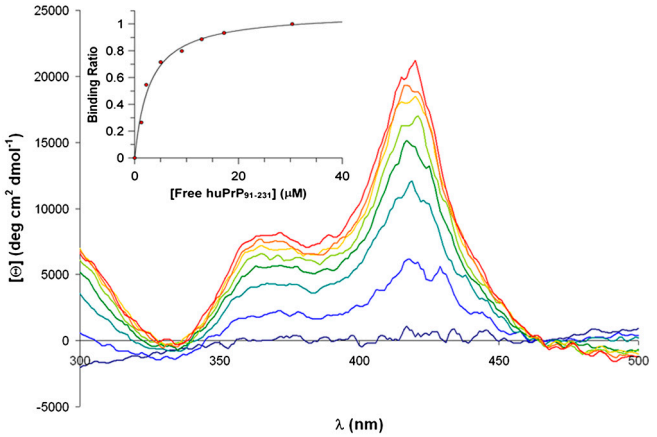

Fig. S2. Induced CD spectroscopy of Fe(III)-TMPyP plus huPrP$_{91–231}$. Induced CD spectra for the addition of huPrP$_{91–231}$ into Fe(III)-TMPyP with the binding isotherm as derived from the average CD signal between 418–423 nm inset.

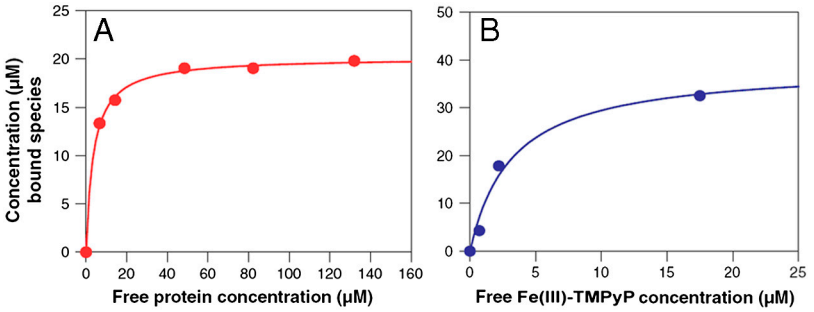

Fig. S3. Analytical ultracentrifugation Fe(III)-TMPyP and huPrP$_{91–231}$. Analytical ultracentrifugation analysis showing the saturation of the huPrP$_{91–231}$:Fe(III)-TMPyP interaction. (*A*) Addition of huPrP$_{91–231}$ into Fe(III)-TMPyP and (*B*) addition of Fe(III)-TMPyP into huPrP$_{91–231}$.

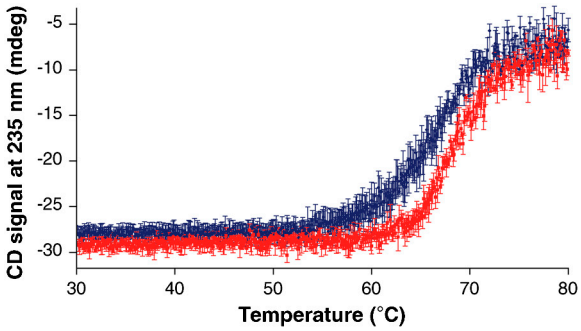

Fig. S4. Effect of Fe(III)-TMPyP on the thermal unfolding and aggregation of huPrP$_{91–231}$. The thermal unfolding/aggregation of huPrP$_{91–231}$ in the presence (red) and absence (blue) of Fe(III)-TMPyP measured by CD spectroscopy at 235 nm.